Crack growth prediction in a thick cylinder under fatigue loading – an FEA

I. Salam, M. Abid, M.A. Malik

Abstract— This paper presents numerical study to predict crack growth rate under fatigue loading in a thick cylinder made of an aluminum alloy. Experimental fatigue crack growth data on middle tension (MT) samples available was applied to simulate and predict crack growth process using detailed 2-dimensional parametric finite element technique. The fatigue crack propagation was simulated based on linear elastic fracture mechanics and stress intensity factor determination. Finite element model provides results of crack growth analysis optimized for the stress levels of 40 to 25 % of the yield stress of the material. Results are plotted on SN curves and the disparity was explained in terms of crack growth rates near threshold stress intensity factor range.

Keywords— Aluminum alloy, fatigue, crack growth, FEA, fracture mechanics.

I. Introduction

Mechanical failure of structures and components is a serious concern in all types of industries. It has been estimated that between 50 to 90 % of these failures are due to fatigue. Fatigue is defined as "The process of progressive localized permanent structural change occurring in a material subjected to conditions that produce fluctuating stresses and strains at some point or points and that may culminate in cracks or complete fracture after a sufficient number of fluctuations" [1]. Fatigue of materials involves a very complex interaction of different metallurgical, mechanical and technological factors and is still only partly understood [2]. These factors include; type frequency and amplitude of load, material model, member size, material flaws, manufacturing method, operating temperature, environmental operating conditions etc. In practice, accurate estimates of fatigue life are difficult to obtain as small changes in these conditions may strongly affect fatigue life and reliance on testing of full-scale members in-service conditions is recommended, which again is very time-consuming and costly. The three major fatigue life methods used in design and analysis are the stress-life method, the strain-life method, and the linear-elastic fracture mechanics (LEFM) method [3]. The numerical techniques based on the linear-elastic fracture mechanics with input data from laboratory tests is often used to establish fatigue failure criteria. In general, the fatigue process is characterized by three distinct regions [3]. Region I is associated with the growth of cracks at low stress intensity factor ranges and is commonly believed to account for a significant proportion of the fatigue life of a component. Region II is the stable crack growth region and has been extensively studied for its technological importance [4]-[17]. Rapid crack growth occurs in region III and this region is typically thought to account for a small fraction of the total life. The typical log-log plot of the da/dN (crack growth rate) versus ΔK (stress intensity factor range) is shown schematically in Fig. 1. The sigmoidal shape can be divided into three major regions. Region I is the near threshold region and exhibits a threshold value, ΔKth, below which there is no observable crack growth. Below ΔKth, fatigue cracks are characterized as non-propagating cracks. Region II normally known as the Paris region shows essentially a linear relationship between log da/dN and log ΔK. This region has received the greatest attention and the Paris equation can be used to model crack propagation in this region. The well known Paris equation is [18];

$$da/dN = C\Delta K^m \quad (1)$$

where, m and C are material constants. Region II fatigue crack growth corresponds to stable macroscopic crack growth. In region III the fatigue crack growth rates are very high as they approach instability, and little fatigue crack growth life is involved. This region is controlled primarily by fracture toughness K_{IC} of the material. In present work, numerical investigations of the crack growth process in a thick walled cylinder made of extruded aluminum alloy [19] under fatigue loading was carried out using detailed 2-D, finite element analysis (FEA). The fatigue crack growth data was collected using middle tension specimens. Dimensions of the MT specimen modeled and analyzed are shown in Fig. 2. The data collected from the experiments was utilized to predict the fatigue life of the samples with the help of numerical technique based on LEFM.

II. FE Modeling, Material Properties, Element Selection and Meshing

Fatigue crack growth analysis was performed using ANSYS software [20]-[21] by repeatedly loading the geometry, recording stress intensity factor K_I at crack tip, advancing the crack and then unloading. Two dimensional finite element analysis of middle tension sample geometry was conducted using 4-noded quadrilateral PLANE42 solid elements under plane-strain condition. An isotropic material for LEFM, with modulus of elasticity E=71000 MPa and Poisson's ratio, ν =0.33 was used [3]. The quarter model with an initial crack length of 3mm, a/W=0.3 was used in FEA due to the symmetry in loading and

Paper submitted March 22, 2007; Revised August 14, 2007

Iftikhar ul Islam is with Department of Mechanical Engineering, College of Electrical and Mechanical Engineering, National University of Sciences & Technology, Rawalpindi, Pakistan. (e-mail: iusalam@yahoo.com).

M. Abid is with GIK Institute of Engineering Sciences and Technology Topi, Pakistan (Corresponding author: phone: 0092-938-271858, fax: 0092-938-271889; e-mail: abid@giki.edu.pk).

M. A. Malik is with Department of Mechanical Engineering, College of Electrical and Mechanical Engineering, National University of Sciences & Technology, Rawalpindi, Pakistan.

geometry of the plate. To predict the crack growth from the crack tip, crack advancing region was mapped meshed. The spacing between the consecutive nodes allowed the crack to advance in steps of equal sizes. The element size along the crack growth line was optimized to obtain the convergence of the results. Mesh with a higher degree of refinement and smaller element size required more load cycles to produce a prescribed amount of crack growth. Meshed model is shown in Fig. 3.

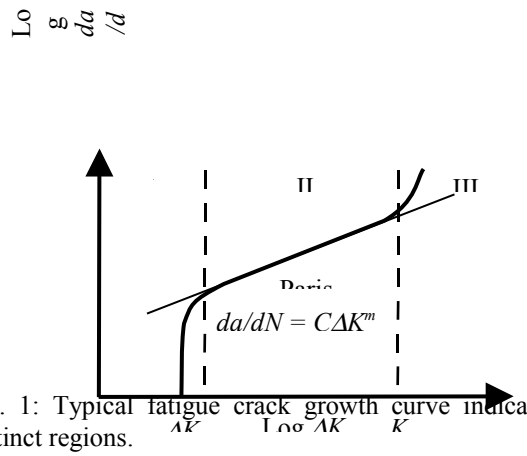

Fig. 1: Typical fatigue crack growth curve indicating three distinct regions.

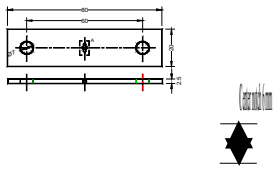

Fig. 2: Dimensional details of the MT sample (dimensions in millimeter).

III. Boundary Conditions

The boundary conditions applied on the MT sample are shown in the figure 4. The half width of model (10mm) was constrained applying symmetry boundary conditions along the left and the bottom edges. A 3mm long crack was modeled by applying no constraints from 0-3mm along the x direction at the bottom edge, thus providing the crack tip node at 3mm. The model was loaded by applying tractions at the upper edge in the y direction, simulating mode I loading. After loading the model and getting the solution, K_{Imax} was obtained at the crack tip, based on which ΔK was calculated. Using experimental data and ΔK value, crack growth rate was calculated using Paris equation. Crack size was increased by releasing the crack tip node, which was equal to the distance between the two consecutive nodes along the line of crack advancement. The number of cycles to move to the next node (one step) was calculated using crack growth rate and the process was repeated. During crack propagation, ΔK value was monitored and the process was stopped as it reached the fracture toughness of the material. Analysis was conducted by applying different loads as applied during the experimental tests to validate FEA results Applied boundary conditions are shown in Fig. 3.

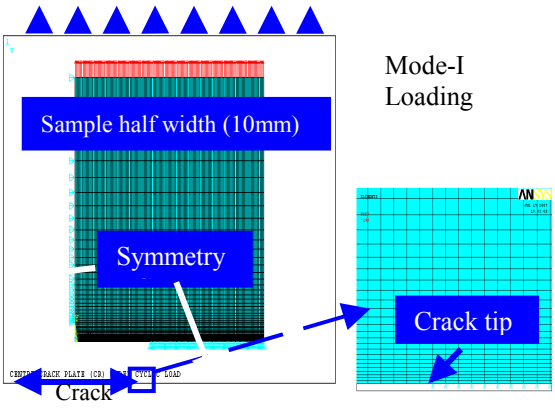

(a) (b)

Fig. 3: a) Quarter model of the MT sample - element plot with applied boundary conditions, b) Crack tip region showing mapped meshing.

IV. Results and Discussion

Fig. 4a shows von Mises stress distribution at stress level of 40% and 1mm crack growth. In Fig. 4b, the crack tip region is enlarged which shows the maximum stress at crack tip node.

V. Element Size Optimization

Before detailed FEA, optimization with element size ranging from 0.01 to 0.5mm concluded that an element size equal to 0.05mm yields optimum results. The conclusion was in agreement with the earlier studies [15]-[16] which concluded that an element size in the neighborhood of 0.05 mm yielded satisfactory stable crack growth predictions under constant amplitude loading. Results of crack size versus number of cycles with different element sizes plotted in Fig. 5 show that by reducing the element size from 0.5 to 0.05mm better convergence was achieved. Further reducing the element size to 0.025mm and 0.01mm did not show any significant difference in the results. Based on these findings, an element size equal to 0.05mm was selected near the crack tip and along the line of crack propagation for further studies.

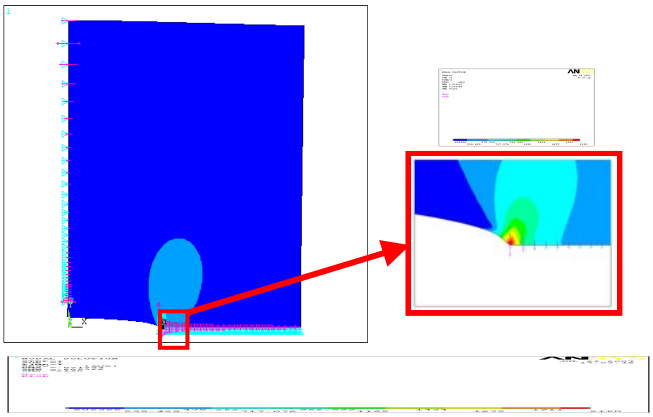

(a) (b)

Fig. 4: a) Von Mises stress distribution at stress level of 40% and crack length 4 mm. b) Crack tip region.

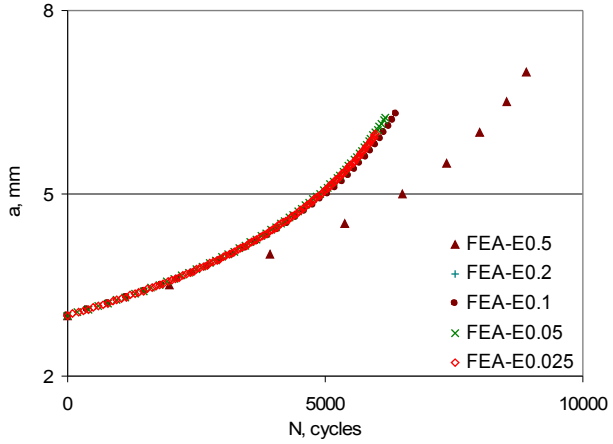

Fig. 5: Element size optimization.

VI. Crack growth

Using optimized element size of 0.05mm, detailed FEA study was performed. The plots in Fig. 6 show FE results of the crack length versus the number of cycles at different stress levels. Data covers the range from start of the crack at the notch up to the specimen failure. From results, it was concluded that crack grows faster at higher stress level and vice versa and validated with the available literature [3]. At lower stress levels, ΔK approaches to ΔK_{th} and enters region I of the fatigue crack growth curve. In this region micro-structural features have greater influence on fatigue crack growth rate [22]. Microstructure has less influence on fatigue crack growth behavior in region II than in region I. The crack growth rate equation is valid only in the stable crack growth region i.e. Paris region. Hence, results presented in this study are concluded optimized for the stress levels giving ΔK values within the Paris regime. However, at lower stress levels the model provides more conservative results. FEA results obtained are compared with the experimental results by Salam et al [19] and are found in good agreement.

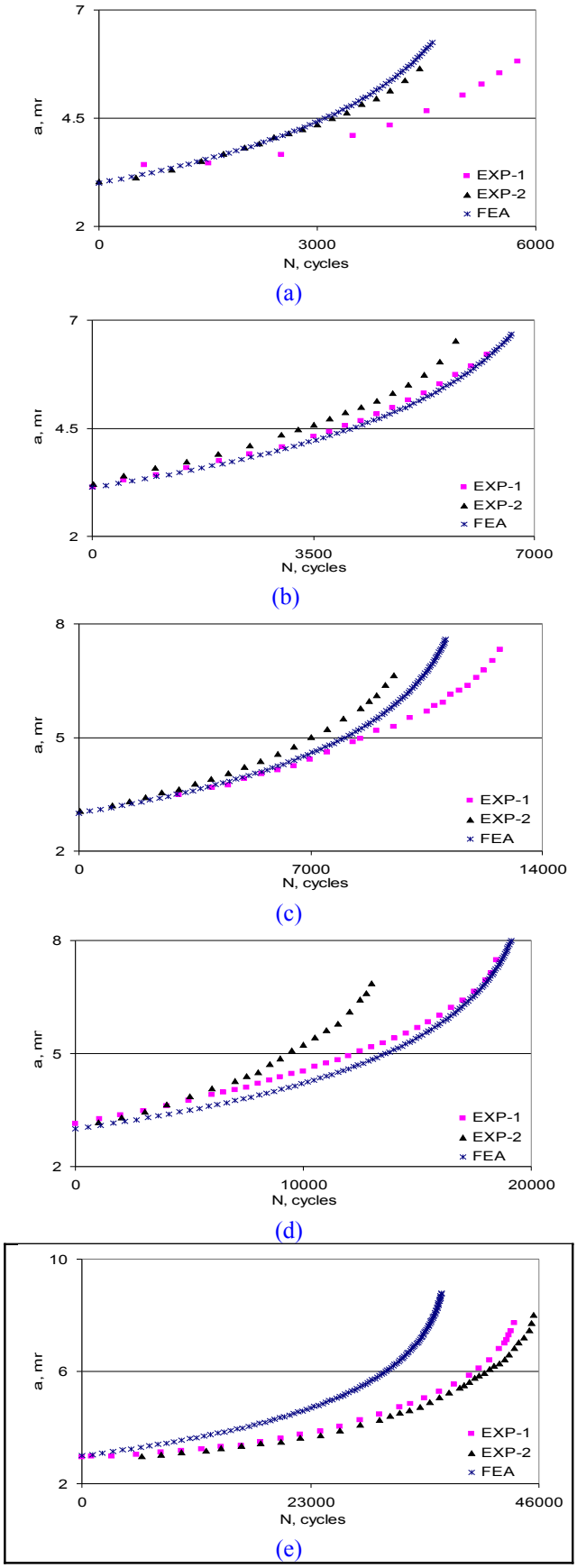

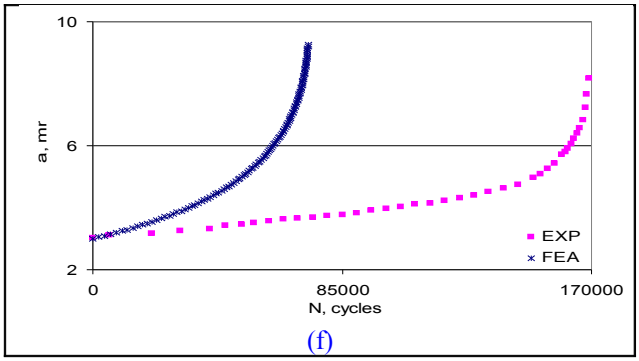

Fig. 6: Experimental and FE results (crack length vs number of cycles at stress levels in % of yield strength). a) 40 b) 35 c) 30 d) 25 e) 20 f) 15.

VII. Predicted Fatigue Crack Growth Rate

The numerical values of the Paris constants obtained are *C=2 E-10* and *m=2.7*. A smooth crack growth rate achieved from the FE analysis is based on the calculation after getting the stress intensity factor during analysis. In order to avoid any deviations a minor adjustment to the value of Paris constant *m* was made. However, the fatigue crack growth rate achieved in FEA with adjusted *m* value was within the upper and lower bounds of the fatigue crack growth rate achieved. Based on the crack extension analysis, as described in the previous section, a straight line is marked on the plot to indicate the value of ΔK that corresponds to the start of Paris region. This value of ΔK is almost 9 MPa.√m.

VIII. Fatigue Life Analysis

FEA results of ΔS versus *Nf* are compared with the available experimental results by Salam et al in Fig. 7. The number of cycles to failure *Nf* includes the cycles to initiate the crack and it's growth up to the specimen failure. The number of cycles to initiate the crack was added in the FE results from the experimental data. SN data from both the techniques shows that the fatigue lifetime increases as the stress range decreases. Based on close agreement FE model is verified up to ΔS equal to 79 MPa. At lower ΔS values *Nf* obtained from FEA lack behind the experimental results and were found 13 and 36 % less at stress ranges of 63 and 49 MPa, respectively. The disparity can be explained in terms of crack growth rates near threshold stress intensity factor range, as discussed earlier.

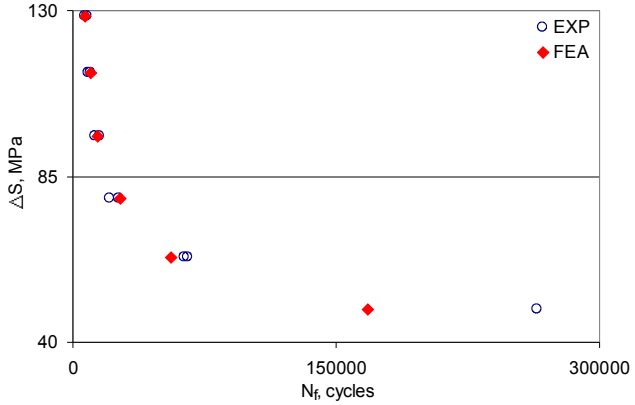

Fig. 7: SN curves: Experimental vs FEA.

IX. Conclusion

From detailed numerical fatigue crack growth study of a high strength aluminum alloy AA 6061-T6 using (MT) specimens, following conclusions are made;

1. In crack growth analysis, FE model provides results optimized for the stress levels of 40 to 25 % of the yield stress. However, at lower stress levels of 15 and 20%, the model provides more conservative results.
2. Fatigue crack growth rate achieved in FEA with adjusted *m* value was within the upper and lower bounds of the fatigue crack growth rate achieved from the experimental data.
3. SN curves from FEA results is verified with the available experimental data up to ΔS equal to 79 MPa. At lower ΔS values *Nf* obtained from FEA lack behind the experimental results and were 13 and 36 % less at ΔS equal to 63 and 49 MPa, respectively.

X. References

[1] Standard Terminology Relating to Fatigue and Fracture, Testing ASTM Designation E1823, Vol. 03.01, ASTM, West Conshohocken, PA, 2000, p. 1034.

[2] Stephens R I, Fatemi A, Stephens R R and Fuchs H O 2001 Metal Fatigue in Engineering, 2nd ed., John Wiley & Sons, Inc., New York

[3] Shigley J E, Mischke C R and Budynas R G 2004 *Mechanical Engineering Design* 7th ed. McGraw-Hill Companies, Inc., New York, NY 10020

[4] Molent L, Jones R, Barter S and Pitt S 2006 *Int. J. Fatigue* **28** 1759–68

[5] Huang X and Moan T 2007 *Int. J. Fatigue* **29** 591–602

[6] Sansoz F and Ghonem H 2003 *Mater. Sci. Eng*. **A356** 81–92

[7] Korda A, Miyashita Y, Mutoh Y and Sadasue T 2007 *Int. J. Fatigue* **29** 1140–48

[8] Ding J, Hall R F, Byrne J and Tong J 2007 *Int. J. Fatigue* **29** 1339–49

[9] Wu F, Ni C, 2006 Eng. Fracture Mech. DOI: 10.1016/j.engfracmech.2006.08.019

[10] Meshii T and Watanabe K 2003 *Nuclear Eng. Design* **220** 285–92

[11] Borrego L P, Ferreira J M, Pinho da Cruz J M and Costa J M 2003 *Eng. Fracture Mech*. **70** 1379–97

[12] Kim J and Shim D 2000 *Int. J. Fatigue* **22** 611–18

[13] Shin C S and Cai C Q 2007 *Int. J. Fatigue* **29** 397–405

[14] Amrouche, Mesmacque G, Garcia S and Talha A 2003 *Int. J. Fatigue* **25** 949–54

[15] Jiang Y and Feng M 2004 In: Fracture Methodologies and Manufacturing Process, uly 25–29, 2004, San Diego, California, ASME PVP-Vol. **474**, PVP2004-2297, 23–31

[16] Ding F, Feng M and Jiang Y 2007 *Int. J. Plasticity* **23** 1167–88

[17] Alam M S and Wahab M A 2005 *Int. J. Pressure Vessels Piping* **82** 105–113

[18] P. C. Paris, M. P. Gomez, and W. E. Anderson, "A Rational Analytical Theory of Fatigue," Trend Eng., Vol. 13, No.9, 1961

[19] Salam I, Malik M A and Muhammad W 2007 *15th International Conference on Nuclear Engineering* (Nagoya, Japan)

[20] ASTM standard E 647 1996 *Annual book of ASTM Standards*. Philadelphia (PA): American Society for Testing and Materials
[21] ANSYS Inc. 2004 *ANSYS Elements Manual* 7th Edition
[22] Nagaralu R 2005 *MS Thesis*, Department of Aerospace Engineering, Mississippi State University